ISSN 0915-633X

NATIONAL INSTITUTE FOR FUSION SCIENCE

Simulation Study of Radial Electric Field in CHS and LHD

S. Murakami, N. Nakajima, U. Gasparino and M. Okamoto

(Received - Dec. 16, 1996)

NIFS-473 Jan. 1997

RESEARCH REPORT
NIFS Series

NAGOYA, JAPAN

Simulation Study of Radial Electric Field in CHS and LHD

S. Murakami, N. Nakajima, U. Gasparino[*], M. Okamoto

National Institute for Fusion Science, Nagoya 464-01, Japan

[*]*Max-Planck-Institut für Plasmaphysik, IPP-EURATOM Association, D-85748 Garching, Germany*

ABSTRACT

The influence of energetic particles generated by various plasma heating methods on the radial electric field is studied numerically in CHS and LHD. The important role played by the radial flux of beam particles during tangentially injected NBI is pointed out in CHS and the strong negative radial electric field experimentally observed near the plasma periphery is reproduced. A strong negative radial electric field, expected to reduce anomalous transport, is found near the plasma periphery in LHD due to the flux of energetic ion generated by ICR heating. On the contrary, a positive radial electric field is obtained by taking into account the energetic electron flux driven by ECR heating in CHS. This can explain the radial electric field transition phenomena observed experimentally.

Keywords : energetic particle, radial electric field, NBI, ICR heating, ECR heating, Compact Helical System, Large Helical Device

1. INTRODUCTION

The radial electric field, E_r, is an important issue for transport improvement in heliotrons. The orbit of ripple trapped particle in heliotrons deviates from the magnetic surface and, thus, E_r can change the trapped particle orbit drastically. For ripple trapped ions negative E_r enlarges the orbit deviation from the magnetic surface while positive E_r or strong negative E_r (i.e. $V_{E\times B} >> V_{\nabla B}$ where $V_{E\times B}$ and $V_{\nabla B}$ are the $E \times B$ and ∇B drift velocities, respectively) reduces the orbit deviation and improve the particle confinement. Consequently the neoclassical diffusion strongly depends on E_r and, therefore, E_r is expected not only to reduce anomalous transport through turbulence suppression but also to reduce neoclassical diffusion in heliotrons.

Because the neoclassical diffusion depends on E_r in non-axisymmetric devices, we can determine E_r by the ambipolarity condition of the neoclassical particle fluxes. The observed E_r have shown agreements with neoclassical estimations[1]. However, recent experiments[2,3] done in Compact Helical System[4] (CHS:l = 2 and m = 8 heliotron/torsatron) have shown negative and positive E_r that can not be simply explained by the neoclassical theory. In these phenomena the radial fluxes enhanced by plasma heating would play an important role and the inclusion of these radial fluxes is necessary for understanding the experimentally observed E_r.

In this paper we study numerically the influence on E_r of the enhanced radial flux by various heating methods (NBI, ICRH, and ECRH) in CHS and Large Helical Device[5] (LHD: l = 2 and m = 10 heliotron/torsatron). The generation of high energetic particles is simulated by realistic NBI, ICR, and ECR heating models and the complex motions of these energetic particles are calculated by Monte Carlo simulations, where we solve the equations of motion in Boozer coordinates based on numerically obtained three dimensional MHD equilibria. We assume that E_r is determined by the ambipolarity condition of neoclassical particle fluxes and particle fluxes of energetic particles, $\Gamma_e^{NC} + \Gamma_e^{fast} = \Gamma_i^{NC} + \Gamma_i^{fast}$, where Γ_s^{NC} and Γ_s^{fast} are the neoclassical radial flux and the particle flux of energetic particles of s-species (electron and ion), respectively. The effect of the anomalous viscosity is also introduced in the plasma periphery in the NBI and ICR heating calculations, in which strong E_r appears near the plasma periphery. Using this simulation model we study the enhancement of E_r by the energetic particle flux generated by various plasma heating methods.

In Sec. 2 the effect of the beam particle flux on E_r is examined in CHS for tangentially injected NBI. By introducing the anomalous viscosity the dependence of the magnitude of E_r on the heating power is studied. The effect of the energetic ion flux driven by ICR heating on E_r is analyzed for LHD in Sec. 3. The possibility to sustain strong negative E_r, expected to reduce anomalous transport, is examined. In Sec. 4 we study the generation of positive E_r by the energetic electron flux driven by ECR heating. The results are compared with the E_r observed in CHS during transition phenomena. Finally, conclusions are given in Sec. 5.

2. ENHANCEMENT OF NEGATIVE E_r BY NBI HEATING IN CHS

A strong negative E_r near the plasma periphery, which can not be explained by neoclassical theory, has been observed in CHS[2]. The origin of this negative E_r has been an unresolved problem[6].

The tangential injection of NBI heating is used to heat the plasma in CHS experiments. In the previous paper[7] we have pointed out that the tangentially injected NBI particles show a large deviation of drift orbits from the original magnetic surface, in a weak magnetic field. The size of the deviation, Δ_d, is given by $\Delta_d = \sigma(\rho_{||}/\iota)\{1 + \sigma 2(\epsilon_0/\epsilon_t)(\rho_{||0}/a\iota_0)\}^{-1}$ with $\sigma = 1$ for the co-injection case and $\sigma = -1$ for the counter-injection case when we assume the simple model magnetic field, B, as $B(r,\theta) = B_0\{1 - \epsilon_t(r/a)\cos\theta + \epsilon_0(r/a)^2\}$. For the CHS parameters (B_0 = 0.9T and beam energy, E_b = 40keV) the size of the deviation becomes $\Delta_d \sim 0.5a$. These large orbit deviations are expected to enhance the radial flux, and, consequently, affect E_r.

In order to evaluate the radial flux due to beam particles, first, we calculate the birth profile of neutral beams using NBI deposition code and, next, the beam particle orbits are followed by taking into account Coulomb collisions with background plasma particles until the beam particles are slowdowned to thermal energy. Then, finally, the radial flux due to beam orbit losses is evaluated using the obtained distribution function of beam particles.

Figure 1 shows the radial flux due to the beam particles for the counter-injection NBI heating for two different densities; n_0 = 2.0 and $6.0 \times 10^{19}\mathrm{m}^{-3}$. The large radial flux due to beam particle, $\Gamma_i^{fast} \geq 1.0 \times 10^{19} 1/\mathrm{sec} \cdot \mathrm{m}^2$ is observed in both density cases. We assumed the heating power of 1MW. It is found that the larger radial flux is observed in the high density case. This is because the shine through loss of neutral beam is smaller for the high density case and, also, as the birth profile of the NBI beam particles moves towards the outer side in the major radius direction due to the larger charge exchange rate. This outer shifted birth profile in the high density case enhances more particle losses for the counter-injection in which the direction of drift orbit shift is toward the inner side in the major radius direction[7]. More than 50% of beam particles are lost by orbit loss in the high density case.

Using the obtained radial fluxes we can evaluate E_r from the ambipolarity condition, $\Gamma_{beam} + \Gamma_i^{NC} = \Gamma_e^{NC}$ where Γ_{beam} is the radial flux of the beam particles, and Γ_i^{NC} and Γ_e^{NC} are radial fluxes of background ions and electrons due to the neoclassical $1/\nu$ ripple diffusion, respectively. Fig. 2-(a) shows the change of E_r due to the NBI beam particle in CHS ($n_0 = 6.0 \times 10^{19}\mathrm{m}^{-3}$). The solid line corresponds to the simulation result while the dashed line to the prediction of neoclassical theory. A slight increase of the negative E_r, compared with neoclassical prediction, is observed in the region $r/a \leq 0.8$ while a strong negative E_r is obtained at the plasma periphery. The magnitude of E_r becomes more than 15kV/m at $r/a \simeq 1$. This is due to the fact that the neoclassical flux goes to 0 at $r/a = 1$. The increase of the negative E_r in the lower density ($n_0 = 2.0 \times 10^{19}\mathrm{m}^{-3}$) is smaller than the case at the higher density. The density dependence of E_r is consistent with the experimental observations[2].

In the actual plasma anomalous transport would play an important role at the plasma periphery. Next we show the effect on the simulation results of an anomalous viscosity in CHS. We, here, introduce the effect of anomalous viscosity and use the ambipolarity condition given by

$$\Gamma_{beam} + \Gamma_i^{NC} - \Gamma_e^{NC} + \frac{1}{V'}\frac{\partial}{\partial \psi}\left(V' D \frac{\partial \Phi'}{\partial \psi}\right) = 0, \quad (1)$$

where Φ and V are the electrostatic potential ($E_r = -\partial\Phi(r)/\partial r$) and the volume enclosed in the flux surface, respectively. We assume $D = D_0 f(r)$ and $f(r) = \{1 + C_1(r/a)^{C_2}\}(C_2 + 2)/(2 + 2C_1 + C_2)$ with $C_1 = 5$ and $C_2 = 8$, so that the effect of anomalous viscosity becomes large near the plasma periphery.

Figure 2-(b) shows the enhancement of E_r in dependence on the NBI heating power in CHS ($n_0 = 6.0 \times 10^{19}\mathrm{m}^{-3}$). In order to estimate the role played by anomalous viscosity we have to compare the strength of the numerically obtained E_r with the experimental one. In the following calculations we fix the value of D_0 in such a way that the strength of the numerically obtained E_r becomes comparable with the experimental one for the case corresponding to the heating power of $P = 1$MW. We can see that the strength of the negative E_r near the plasma periphery increases with the increase of the heating power.

Additionally the radial width of the region with the strongly enhanced E_r also increases with the heating power. The poloidal $E \times B$ Mach number, $M_p = V_{E\times B}B/v_{th}B_p$, is a good measure to evaluate the effect of the obtained E_r on anomalous transport where v_{th} and B_p are the ion thermal velocity and the poloidal magnetic field, respectively. It is found that the heating power of 2MW is required in order to achieve $M_p \sim 2$ for which sudden changes of E_r would be observed[8,9].

3. ENHANCEMENT OF NEGATIVE E_r BY ICR HEATING IN LHD

Tangentially injected NBI, P = 15MW and beam energy E_b = 180keV, is being prepared also in LHD. However the size of the orbit deviation for LHD (B_0 = 3.0T) is small, $\Delta_d \leq 0.1a$ and the beam particles are well confined. Therefore the beam particle flux due to tangential NBI heating is not expected to be effective in order to enhance E_r in LHD.

High power ICR heating scenario, $P \geq$ 12MW, is also planed in LHD. ICR heating produces energetic trapped particles, whose motions can be very complicated in heliotrons. The loss of these energetic particles would enhance the radial flux, leading to an enhancement of E_r. Figure 3 shows the heating efficiency as a function of heating power (solid line) obtained by Monte Carlo simulation[10]. We set Z_{eff} = 1.3 and the parameters at the plasma center as $n_0 = 1.0 \times 10^{20}\mathrm{m}^{-3}$, T_{e0} = 1.0keV, and T_{i0} = 1.0keV. We assume 3% of proton minority ion fraction in a deuteron plasma. We can see the decrease of heating efficiency as the heating power increases. Thus, the loss flux of high energetic ions increases with heating power and the driven radial flux would enhance the negative E_r.

In this section we study the influence of energetic minority ions generated by ICR heating on E_r. Because E_r affects the orbit of fast ion while the escaping fast ion flux alters E_r itself, the orbit of fast ions and E_r have to be evaluated self-consistently. In order to obtain the self-consistent solution of the ambipolarity condition we use the equation for the time development of E_r[11] as

$$\frac{\partial}{\partial t}\epsilon_\perp E_r = e\Gamma_e - eZ_i\Gamma_i - eZ_f\Gamma_f + \frac{1}{V'}\frac{\partial}{\partial\psi}\left(V'D\frac{\partial\Phi'}{\partial\psi}\right). \tag{2}$$

The ambipolarity condition is obtained as the steady state solution of this equation where Γ_e and Γ_i are the radial particle fluxes for electrons and majority ions, and Γ_f is related to the loss of minority ions, respectively. The same anomalous viscosity term as the one used in the previous NBI calculation is also introduced in this calculation and we assume the same value for D_0. Γ_e and Γ_i are calculated by the neoclassical theory and Γ_f by the Monte Carlo simulation code.

Figure 4 shows the time development of the radial electric field and of the electrostatic potential during the ICRF heating with P_{abs} = 7.5MW and same plasma parameters as in Fig. 3. We find an enhancement of the strong negative E_r at the periphery due to the radial flux of energetic minority ions escaping out of the last closed magnetic surface. The maximum value of the strength of E_r reaches to 110kV/m and we can obtain a plasma with $M_p > 2$ using ICR heating. The enhancement of E_r is larger for higher β plasma due to the large loss region of energetic ions. We can also find an improvement in the heating efficiency of more than 10%, compared with the case where no radial electric field is present (The diamond in Fig. 3 shows the heating efficiency with self-consistent E_r).

4. GENERATION OF POSITIVE E_r BY ECR HEATING IN CHS

Positive E_r reduces the deviation of ripple trapped ion from the magnetic surface and, thus, improves trapped ion confinement and neoclassical transport. It is observed that E_r suddenly changes from negative to positive when ECR waves are applied to low density NBI heated plasma[3]. Ripple trapped energetic electrons are created during ECR heating and their drift motions across the magnetic surfaces can play an important role in these phenomena. The effect of energetic electron drift motions on the broadening of radial heating profile is also pointed out in W7-AS[12].

We have developed a Monte Carlo simulation code[13,14] based on a technique similar to the adjoint equation for dynamic linearized problems[15]. The linearized drift kinetic equation for the deviation from the Maxwellian background $f_1(\underline{x}, \underline{v})$,

$$\vec{v} \cdot \nabla f_1 + \vec{a} \cdot \nabla_v f_1 = C(f_1) + S_{ql}^0, \tag{3}$$

is solved where $C(f_1)$ is the linear Coulomb collision operator and S_{ql}^0 is the wave induced flux in velocity space (quasi-linear diffusion term) which is assumed to be a given function.

Figure 5-(a) shows the radial profile of the enhanced electron radial flux driven by the ECR heating (X-mode 2nd-harmonic) in CHS ($n_0 = 1.0 \times 10^{19}\mathrm{m}^{-3}$). The temperatures are set to 400eV for electrons and 200eV for ions (ECR and NBI combined heating). We assume the heating point to be in the low field side of the toroidal field (the outer side of the major radius) on a vertically elongated cross section at the radial point, $r/a = 0.5$,

which corresponds to the bottom heating case in the CHS experiments[3]. The quasi-linear diffusion term S^0_{ql} is estimated through an analytical model of ECR heating. The previously obtained enhanced radial flux due to beam particles by NBI heating (P = 1MW) is also shown. We can see that the enhanced electron flux driven by ECR heating becomes almost half of the beam enhanced flux even for much smaller heating power. The obtained radial flux is comparable or larger than the neoclassical one and it could affect the radial electric field.

Figure 5-(b) shows the response of E_r ($n_0 = 1.0 \times 10^{19}\mathrm{m}^{-3}$) to changes in the ECR heating power and, consequently, the enhanced radial electron flux. The ambipolarity condition is used to determine E_r. We can see that a positive E_r appears in the region $r/a > 0.6$ when the ECR heating power is increased. Maximum E_r strength is observed at $r/a \simeq 0.8$. It is found that, for significant heating power, the large enhanced radial flux driven by ECR heating can change the E_r profile and, consequently, that the enhanced electron flux play an important role in explaining the experimentally observed E_r transition phenomena[3].

5. CONCLUSIONS

We have shown in the present study that the energetic particles created by various plasma heating methods can affect the radial electric field in CHS and LHD. The enhanced radial flux due to tangentially injected NBI beams can generate strong negative radial electric field near the plasma periphery, as observed in CHS experiments. Although the enhanced radial flux due to the beam particles is not expected to be enough to enhance the negative radial electric field in LHD, we have demonstrated that energetic ion flux generated by ICR heating can be used to generate the strong negative radial electric field in LHD.

Simulations with anomalous viscosity have shown that about 2MW of NBI(ctr.) power is required in CHS and 7.5MW of ICRH power is sufficient in LHD for obtaining the poloidal Mach number $M_p \geq 2$ where we can expect the transition of radial electric field. More detailed calculations including the nonlinear viscosity term[7] are necessary to predict the transition of the radial electric field in CHS and LHD.

The generation of positive radial electric field due to the energetic electrons driven by ECR heating has been shown. The radial drift of ripple trapped electrons generates a large radial flux which can explain the generation of positive radial electric field as observed in the CHS experiment. This creation of a positive radial electric field would have beneficial effects on the neoclassical transport in the long-mean-free-path regimes. The possibility of the generation of a positive radial electric field in LHD is now under investigation.

ACKNOWLEDGMENTS

The authors acknowledge to the members of CHS Group and Heating Group at the National Institute for Fusion science.

REFERENCES

[1] Kühner, G., et al., in Plasma Physics and Controlled Nuclear Fusion Research 1994 (Proc. 15th Int. Conf. Sevilla, 1994), Vol. 1, IAEA, Vienna (1995) 145.

[2] Ida, K., et al., Phys. Fluids B **3** (1991) 515.

[3] Idei, H., et al., Phys. Plasmas **1** (1994) 3400.

[4] Nishimura, K., et al, Fusion Technol. **17** (1990) 86.

[5] Iiyoshi, A., et al., Fusion Technol. **17** (1990) 148.

[6] Sanuki, H., Itoh, K., Ida, K., Itoh, S-I., J. Phys. Soc. Japan **60** (1991) 3698.

[7] Murakami, S., Nakajima, N., Okamura, S., Okamoto, M., Nuclear Fusion **36** (1996) 359.

[8] Shaing, K.C., Phys. Fluids B**5** (1993) 3841.

[9] Yokoyama, M., et al., Nuclear Fusion **35** (1995) 153.

[10] Murakami, S., Okamoto, M, Nakajima, N., Ohnishi, M, and Okada, H., Nucl. Fusion **34** (1994) 913.

[11] Murakami, S., et al., in Plasma Physics and Controlled Nuclear Fusion Research 1994 (Proc. 15th Int. Conf. Sevilla, 1994), Vol. 3, IAEA, Vienna (1995) 531.

[12] Romé, M., et al, to be published in Plasma Phys. Control. Fusion.

[13] Murakami, S., et al., to be published in Proc. Int. Conf. Plasma Phys. 1996 Nagoya, 9I02.

[14] Murakami, S., Nakajima, N., Okamura, S., Gasparino, U., Okamoto, M., to be published in Plasma Physics and Controlled Nuclear Fusion Research 1996 (Proc. 16th Int. Conf. Montreal, 1996), IAEA-CN-64/CP-6.

[15] Fisch, N. J., Phys. Fluids **29** (1986) 172.

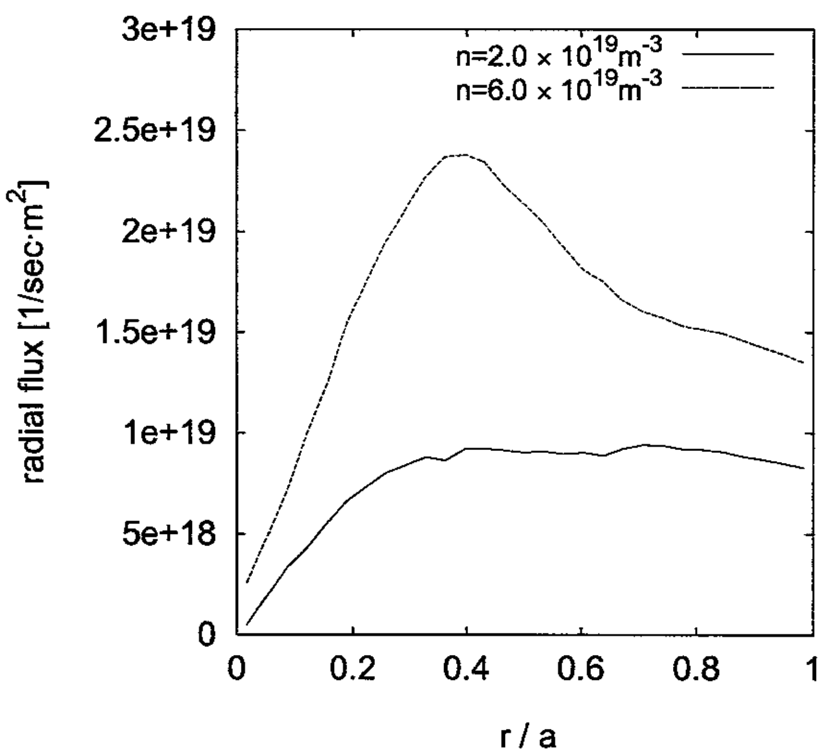

Fig. 1 : Radial flux due to energetic beam particles (counter injection NBI heating, P = 1MW) in CHS for two different densities [n_0 = 2.0 and 6.0 × $10^{19}m^{-3}$].

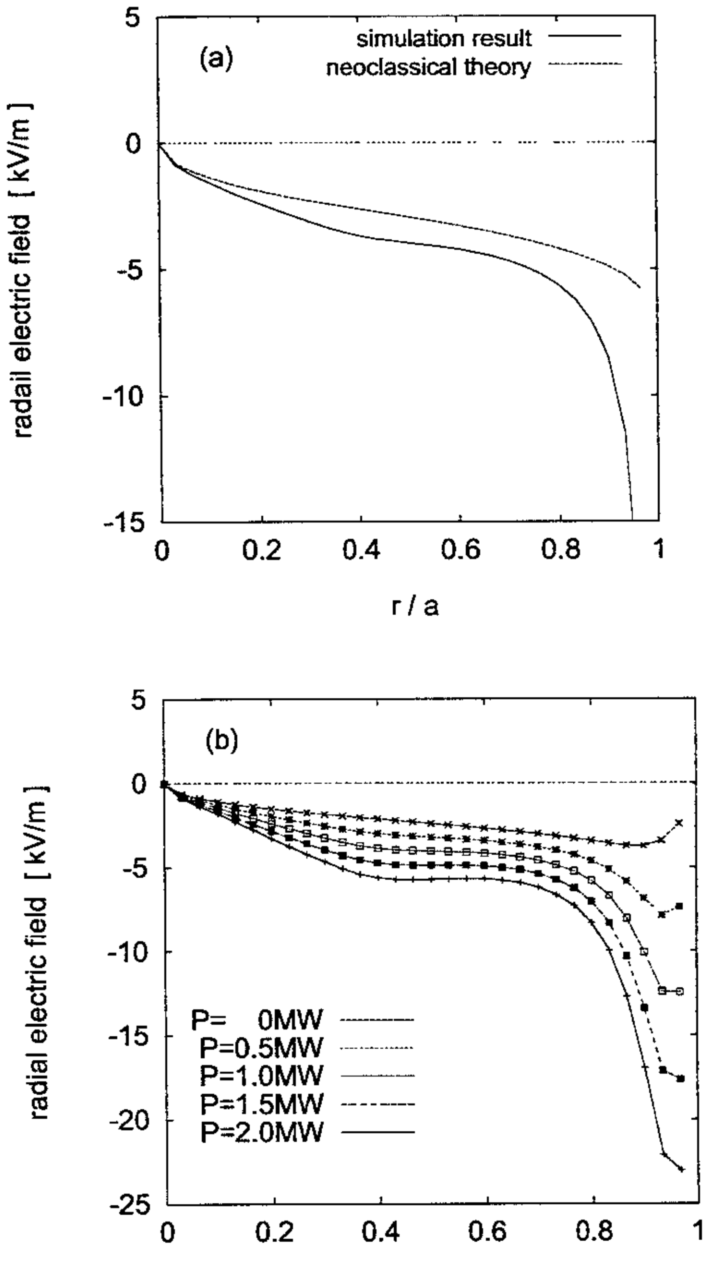

Fig. 2 : (a) Change of the radial electric field due to the radial flux of NBI beam particles (counter injection NBI heating, P = 1MW) in CHS ; simulation results (solid line) and neoclassical theory (dashed line). [$n_0 = 6.0 \times 10^{19} \mathrm{m}^{-3}$] (b) Radial electric field enhancement with anomalous viscosity effect with different NBI heating power.

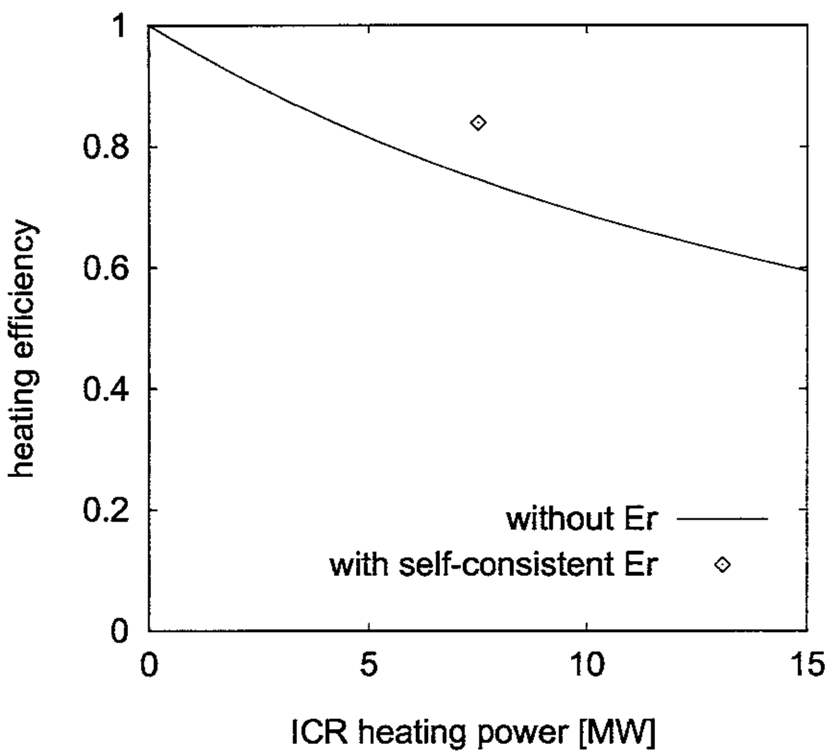

Fig. 3 : Heating efficiency as a function of absorbed ICR heating power without E_r (solid line) and with self-consistent E_r (diamond).

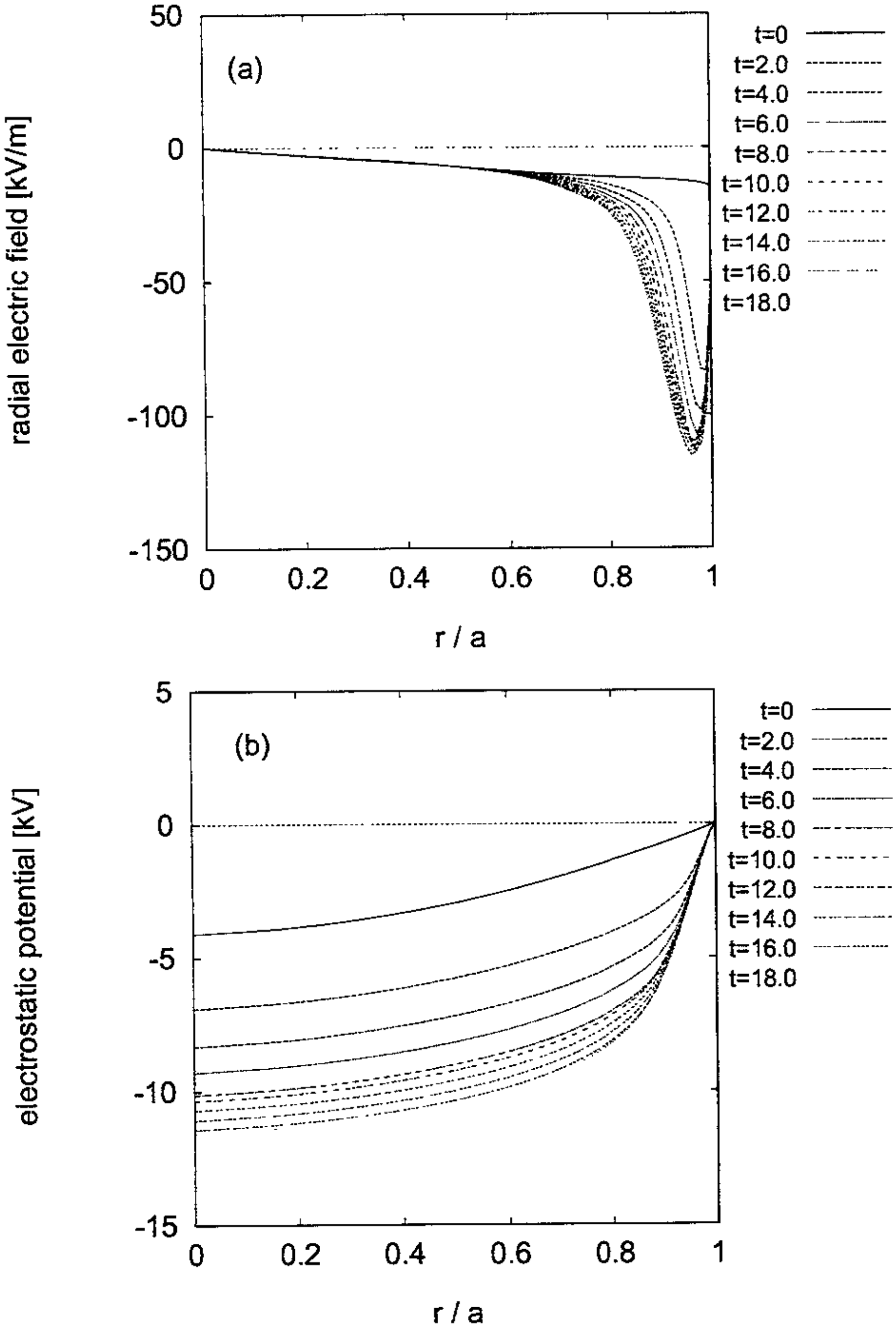

Fig. 4 : Build up of the radial electric field (a) and of the electrostatic potential (b) due to the enhanced radial flux of energetic minority ions generated by ICR heating in LHD.

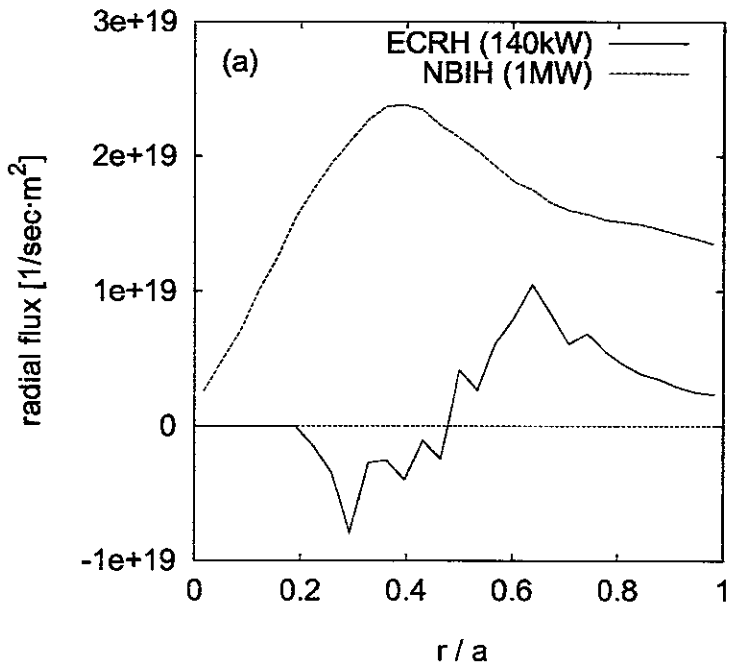

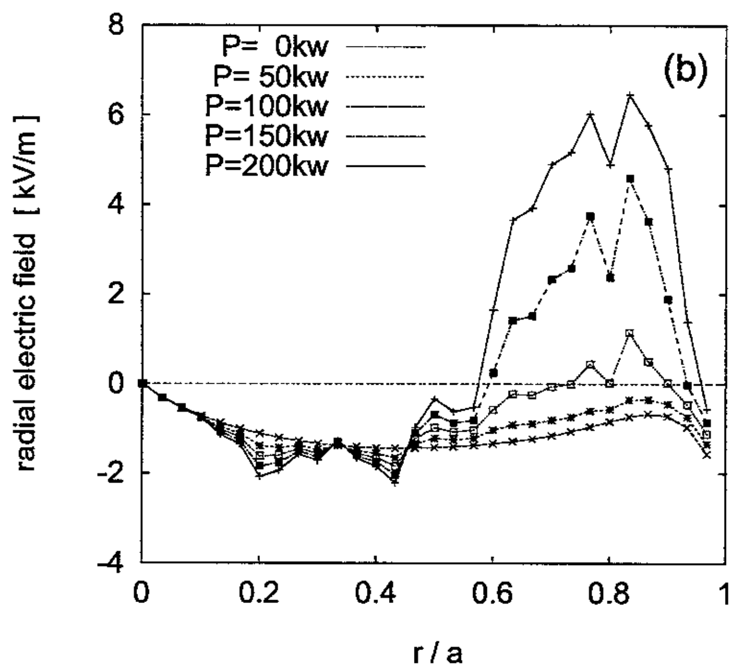

Fig. 5 : (a) Radial fluxes due to energetic electrons by ECR heating (140kW) and due to beam particles by NBI heating (1MW). (b) Dependence of E_r on the ECR heating power.

Recent Issues of NIFS Series

NIFS-434 Y. Suzuki, K. Kusano and K. Nishikawa,
Three-Dimensional Simulation Study of the Magnetohydrodynamic Relaxation Process in the Solar Corona. II.; Aug. 1996

NIFS-435 H. Sugama and W. Horton,
Transport Processes and Entropy Production in Toroidally Rotating Plasmas with Electrostatic Turbulence; Aug. 1996

NIFS-436 T. Kato, E. Rachlew-Källne, P. Hörling and K.-D Zastrow,
Observations and Modelling of Line Intensity Ratios of OV Multiplet Lines for 2s3s 3S1 - 2s3p 3Pj; Aug. 1996

NIFS-437 T. Morisaki, A. Komori, R. Akiyama, H. Idei, H. Iguchi, N. Inoue, Y. Kawai, S. Kubo, S. Masuzaki, K. Matsuoka, T. Minami, S. Morita, N. Noda, N. Ohyabu, S. Okamura, M. Osakabe, H. Suzuki, K. Tanaka, C. Takahashi, H. Yamada, I. Yamada and O. Motojima,
Experimental Study of Edge Plasma Structure in Various Discharges on Compact Helical System; Aug. 1996

NIFS-438 A. Komori, N. Ohyabu, S. Masuzaki, T. Morisaki, H. Suzuki, C. Takahashi, S. Sakakibara, K. Watanabe, T. Watanabe, T. Minami, S. Morita, K. Tanaka, S. Ohdachi, S. Kubo, N. Inoue, H. Yamada, K. Nishimura, S. Okamura, K. Matsuoka, O. Motojima, M. Fujiwara, A. Iiyoshi, C. C. Klepper, J.F. Lyon, A.C. England, D.E. Greenwood, D.K. Lee, D.R. Overbey, J.A. Rome, D.E. Schechter and C.T. Wilson,
Edge Plasma Control by a Local Island Divertor in the Compact Helical System; Sep. 1996 (IAEA-CN-64/C1-2)

NIFS-439 K. Ida, K. Kondo, K. Nagaski T. Hamada, H. Zushi, S. Hidekuma, F. Sano, T. Mizuuchi, H. Okada, S. Besshou, H. Funaba, Y. Kurimoto, K. Watanabe and T. Obiki,
Dynamics of Ion Temperature in Heliotron-E; Sep. 1996 (IAEA-CN-64/CP-5)

NIFS-440 S. Morita, H. Idei, H. Iguchi, S. Kubo, K. Matsuoka, T. Minami, S. Okamura, T. Ozaki, K. Tanaka, K. Toi, R. Akiyama, A. Ejiri, A. Fujisawa, M. Fujiwara, M. Goto, K. Ida, N. Inoue, A. Komori, R. Kumazawa, S. Masuzaki, T. Morisaki, S. Muto, K. Narihara, K. Nishimura, I. Nomura, S. Ohdachi, M.. Osakabe, A. Sagara, Y. Shirai, H. Suzuki, C. Takahashi, K. Tsumori, T. Watari, H. Yamada and I. Yamada,
A Study on Density Profile and Density Limit of NBI Plasmas in CHS; Sep. 1996 (IAEA-CN-64/CP-3)

NIFS-441 O. Kaneko, Y. Takeiri, K. Tsumori, Y. Oka, M. Osakabe, R. Akiyama, T. Kawamoto, E. Asano and T. Kuroda,
Development of Negative-Ion-Based Neutral Beam Injector for the Large Helical Device; Sep. 1996 (IAEA-CN-64/GP-9)

NIFS-442 K. Toi, K.N. Sato, Y. Hamada, S. Ohdachi, H. Sakakita, A. Nishizawa, A. Ejiri, K. Narihara, H. Kuramoto, Y. Kawasumi, S. Kubo, T. Seki, K. Kitachi, J. Xu, K. Ida, K. Kawahata, I. Nomura, K. Adachi, R. Akiyama, A. Fujisawa, J. Fujita, N. Hiraki, S. Hidekuma, S. Hirokura, H. Idei, T. Ido, H. Iguchi, K. Iwasaki, M. Isobe, O. Kaneko, Y. Kano, M. Kojima, J. Koog, R. Kumazawa, T. Kuroda, J. Li, R. Liang, T. Minami, S. Morita, K. Ohkubo, Y. Oka, S. Okajima, M. Osakabe, Y. Sakawa, M. Sasao, K. Sato, T. Shimpo, T. Shoji, H. Sugai, T. Watari, I. Yamada and K. Yamauti,
Studies of Perturbative Plasma Transport, Ice Pellet Ablation and Sawtooth Phenomena in the JIPP T-IIU Tokamak; Sep. 1996 (IAEA-CN-64/A6-5)

NIFS-443 Y. Todo, T. Sato and The Complexity Simulation Group,
Vlasov-MHD and Particle-MHD Simulations of the Toroidal Alfvén Eigenmode; Sep. 1996 (IAEA-CN-64/D2-3)

NIFS-444 A. Fujisawa, S. Kubo, H. Iguchi, H. Idei, T. Minami, H. Sanuki, K. Itoh, S. Okamura, K. Matsuoka, K. Tanaka, S. Lee, M. Kojima, T.P. Crowley, Y. Hamada, M. Iwase, H. Nagasaki, H. Suzuki, N. Inoue, R. Akiyama, M. Osakabe, S. Morita, C. Takahashi, S. Muto, A. Ejiri, K. Ida, S. Nishimura, K. Narihara, I. Yamada, K. Toi, S. Ohdachi, T. Ozaki, A. Komori, K. Nishimura, S. Hidekuma, K. Ohkubo, D.A. Rasmussen, J.B. Wilgen, M. Murakami, T. Watari and M. Fujiwara,
An Experimental Study of Plasma Confinement and Heating Efficiency through the Potential Profile Measurements with a Heavy Ion Beam Probe in the Compact Helical System; Sep. 1996 (IAEA-CN-64/C1-5)

NIFS-445 O. Motojima, N. Yanagi, S. Imagawa, K. Takahata, S. Yamada, A. Iwamoto, H. Chikaraishi, S. Kitagawa, R. Maekawa, S. Masuzaki, T. Mito, T. Morisaki, A. Nishimura, S. Sakakibara, S. Satoh, T. Satow, H. Tamura, S. Tanahashi, K. Watanabe, S. Yamaguchi, J. Yamamoto, M.Fujiwara and A. Iiyoshi,
Superconducting Magnet Design and Construction of LHD; Sep. 1996 (IAEA-CN-64/G2-4)

NIFS-446 S. Murakami, N. Nakajima, S. Okamura, M. Okamoto and U. Gasparino,
Orbit Effects of Energetic Particles on the Reachable β–Value and the Radial Electric Field in NBI and ECR Heated Heliotron Plasmas; Sep. 1996 (IAEA-CN-64/CP -6) Sep. 1996

NIFS-447 K. Yamazaki, A. Sagara, O. Motojima, M. Fujiwara, T. Amano, H. Chikaraishi, S. Imagawa, T. Muroga. N. Noda, N. Ohyabu, T. Satow, J.F. Wang, K.Y. Watanabe, J. Yamamoto , H. Yamanishi, A. Kohyama, H. Matsui, O. Mitarai, T. Noda, A.A. Shishkin, S. Tanaka and T. Terai
Design Assessment of Heliotron Reactor; Sep. 1996 (IAEA-CN-64/G1-5)

NIFS-448 M. Ozaki, T. Sato and the Complexity Simulation Group,
Interactions of Convecting Magnetic Loops and Arcades; Sep. 1996

NIFS-449 T. Aoki,
Interpolated Differential Operator (IDO) Scheme for Solving Partial Differential Equations; Sep. 1996

NIFS-450 D. Biskamp and T. Sato,
Partial Reconnection in the Sawtooth Collapse; Sep. 1996

NIFS-451 J. Li, X. Gong, L. Luo, F.X. Yin, N. Noda, B. Wan, W. Xu, X. Gao, F. Yin, J.G. Jiang, Z Wu., J.Y Zhao, M. Wu, S. Liu and Y. Han,
Effects of High Z Probe on Plasma Behavior in HT-6M Tokamak; Sep. 1996

NIFS-452 N. Nakajima, K. Ichiguchi, M. Okamoto and R.L. Dewar,
Ballooning Modes in Heliotrons/Torsatrons; Sep. 1996 (IAEA-CN-64/D3-6)

NIFS-453 A. Iiyoshi,
Overview of Helical Systems; Sep. 1996 (IAEA-CN-64/O1-7)

NIFS-454 S. Saito, Y. Nomura, K. Hirose and Y.H. Ichikawa,
Separatrix Reconnection and Periodic Orbit Annihilation in the Harper Map; Oct. 1996

NIFS-455 K. Ichiguchi, N. Nakajima and M. Okamoto,
Topics on MHD Equilibrium and Stability in Heliotron / Torsatron; Oct. 1996

NIFS-456 G. Kawahara, S. Kida, M. Tanaka and S. Yanase,
Wrap, Tilt and Stretch of Vorticity Lines around a Strong Straight Vortex Tube in a Simple Shear Flow; Oct. 1996

NIFS-457 K. Itoh, S.- I. Itoh, A. Fukuyama and M. Yagi,
Turbulent Transport and Structural Transition in Confined Plasmas; Oct. 1996

NIFS-458 A. Kageyama and T. Sato,
Generation Mechanism of a Dipole Field by a Magnetohydrodynamic Dynamo; Oct. 1996

NIFS-459 K. Araki, J. Mizushima and S. Yanase,
The Non-axisymmetric Instability of the Wide-Gap Spherical Couette Flow; Oct. 1996

NIFS-460 Y. Hamada, A. Fujisawa, H. Iguchi, A. Nishizawa and Y. Kawasumi,
A Tandem Parallel Plate Analyzer; Nov. 1996

NIFS-461 Y. Hamada, A. Nishizawa, Y. Kawasumi, A. Fujisawa, K. Narihara, K. Ida, A. Ejiri, S. Ohdachi, K. Kawahata, K. Toi, K. Sato, T. Seki, H. Iguchi, K. Adachi, S. Hidekuma, S.Hirokura, K. Iwasaki, T. Ido, M. Kojima, J. Koong, R. Kumazawa, H. Kuramoto, T. Minami, I. Nomura, H. Sakakita, M. Sasao, K.N. Sato, T. Tsuzuki, J. Xu, I. Yamada and T. Watari,
Density Fluctuation in JIPP T-IIU Tokamak Plasmas Measured by a Heavy Ion Beam Probe; Nov. 1996

NIFS-462 N. Katsuragawa, H. Hojo and A. Mase, *Simulation Study on Cross Polarization Scattering of Ultrashort-Pulse Electromagnetic Waves*; Nov. 1996

NIFS-463 V. Voitsenya, V. Konovalov, O. Motojima, K. Narihara, M. Becker and B. Schunke, *Evaluations of Different Metals for Manufacturing Mirrors of Thomson Scattering System for the LHD Divertor Plasma*; Nov. 1996

NIFS-464 M. Pereyaslavets, M. Sato, T. Shimozuma, Y. Takita, H. Idei, S. Kubo, K. Ohkubo and K. Hayashi, *Development and Simulation of RF Components for High Power Millimeter Wave Gyrotrons*; Nov. 1997

NIFS-465 V.S. Voitsenya, S. Masuzaki, O. Motojima, N. Noda and N. Ohyabu, *On the Use of CX Atom Analyzer for Study Characteristics of Ion Component in a LHD Divertor Plasma*; Dec. 1996

NIFS-466 H. Miura and S. Kida, *Identification of Tubular Vortices in Complex Flows*; Dec. 1996

NIFS-467 Y. Takeiri, Y. Oka, M. Osakabe, K. Tsumori, O. Kaneko, T. Takanashi, E. Asano, T. Kawamoto, R. Akiyama and T. Kuroda, *Suppression of Accelerated Electrons in a High-current Large Negative Ion Source*; Dec. 1996

NIFS-468 A. Sagara, Y. Hasegawa, K. Tsuzuki, N. Inoue, H. Suzuki, T. Morisaki, N. Noda, O. Motojima, S. Okamura, K. Matsuoka, R. Akiyama, K. Ida, H. Idei, K. Iwasaki, S. Kubo, T. Minami, S. Morita, K. Narihara, T. Ozaki, K. Sato, C. Takahashi, K. Tanaka, K. Toi and I. Yamada, *Real Time Boronization Experiments in CHS and Scaling for LHD*; Dec. 1996

NIFS-469 V.L. Vdovin, T.Watari and A. Fukuyama, *3D Maxwell-Vlasov Boundary Value Problem Solution in Stellarator Geometry in Ion Cyclotron Frequency Range (final report)*; Dec. 1996

NIFS-470 N. Nakajima, M. Yokoyama, M. Okamoto and J. Nührenberg, *Optimization of M=2 Stellarator*; Dec. 1996

NIFS-471 A. Fujisawa, H. Iguchi, S. Lee and Y. Hamada, *Effects of Horizontal Injection Angle Displacements on Energy Measurements with Parallel Plate Energy Analyzer*; Dec. 1996

NIFS-472 R. Kanno, N. Nakajima, H. Sugama, M. Okamoto and Y. Ogawa, *Effects of Finite-β and Radial Electric Fields on Neoclassical Transport in the Large Helical Device;* Jan. 1997

NIFS-473 S. Murakami, N. Nakajima, U. Gasparino and M. Okamoto, *Simulation Study of Radial Electric Field in CHS and LHD*; Jan. 1997